Correlation Between Core and Pedestal Temperatures in JT-60U: Experiment and Modeling

D. R. MIKKELSEN, Princeton Plasmas Physics Laboratory; E-mail: mikk@pppl.gov

H. SHIRAI, N. ASAKURA, T. FUJITA, T. FUKUDA, T. HATAE, S. IDE, A. ISAYAMA, Y. KAMADA, Y. KAWANO, Y. KOIDE, O. NAITO, Y. SAKAMOTO, T. TAKIZUKA, JAERI Naka Fusion Research Establishment

H. URANO, Hokkaido University

The 'stiffness' of thermal transport in ELMy H-modes is explored in a series of carefully chosen JT-60U plasmas and with temperature predictions based on several transport models. Four scans of pedestal temperature, T_{ped}, with constant heating power and one heating power scan with constant T_{ped} are presented. We find that 30-80% increases in T_{ped} are associated with 10-70% increases in core temperature even though the total heating power is constant. Increasing the heating power by 45% gives almost the same core temperatures (and a 12% density increase) in a group of five plasmas with the same pedestal temperature. The results can be characterized as having relatively 'soft' transport in the plasma periphery and relatively 'stiff' transport in the core. Another series of experiments varied the heating in the deep core by employing different groups of neutral beams that deposit their power on-axis and off-axis. In these plasmas on-axis heating produces systematically more peaked temperature profiles; the rise from the periphery to the central region is ~20% higher in plasmas that have 60% more heating power inside r=a/2. Transport models are tested by solving the power balance equations to predict temperatures, which are then compared to the measurements. The RLWB and IFS/PPPL models' predictions generally agree with the measured temperatures, but the Multimode model uniformly predicts temperatures that are too high except for the central sawtoothing region.

1. Introduction

Predictions of ITER performance depend strongly on the 'stiffness' of the assumed transport model [1, 2]. Previous tests of transport models found that several models - of varying stiffness - were equivalently successful in representing a wide range of tokamak plasmas [1, 2]. We describe plasmas which exhibit profile 'stiffness', and we test the ability of several transport models to account for the linkage between core and peripheral temperatures observed in JT-60U ELMy H-mode plasmas [3,4].

Previous tests of transport stiffness based on transient phenomena led to new insights, but no transport model was clearly successful [7]. The tests presented here use the stationary power balance to directly address the defining characteristic of stiffness: large changes in conducted power are accommodated by smaller changes in the ion temperature gradient scale length, L_{Ti}, when near the critical L_{Ti}. When pedestal temperature and heating power are independently varied we observe a strong correlation between core and peripheral temperatures, largely independent of the heating power. Core-pedestal temperature linkage has also been observed in ASDEX-U [6] and C-mod [7], so similar experiments may be possible in these devices.

Transport models are tested by solving electron and ion power balance equations to make temperature predictions for a number of the discharges described below. Predictions of all three tested models qualitatively resemble the observed linkage between core and peripheral temperatures. The IFS/PPPL and RLWB models predict temperatures that are within ~15% in the 'confinement region', $0.3 < r/a < 0.7$, but the Multimode model uniformly predicts too high a temperature except in the sawtoothing region.

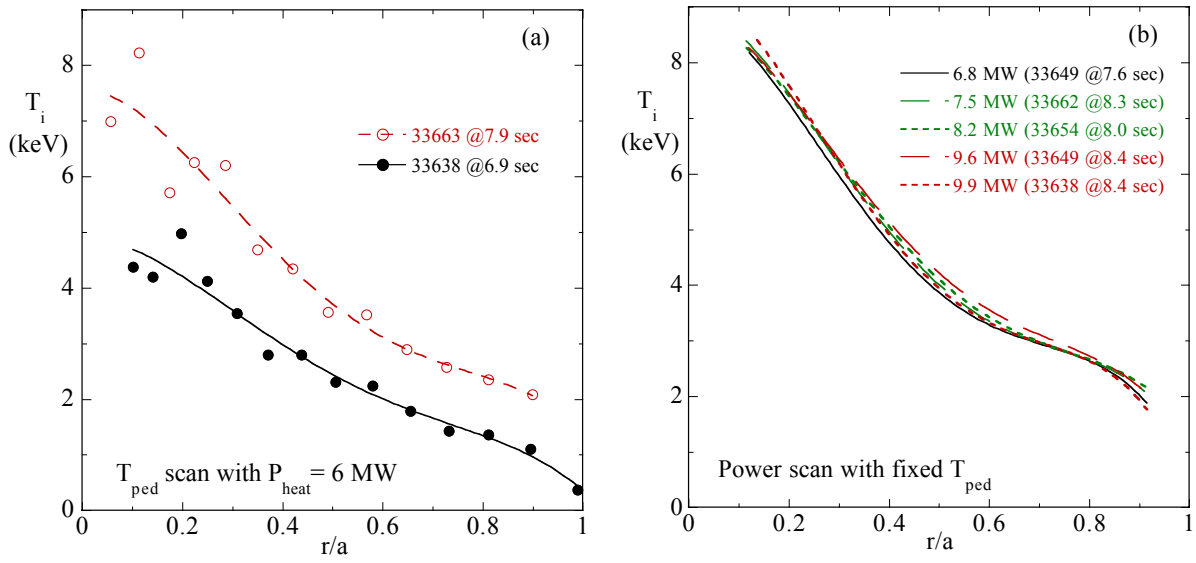

Fig.1. a) Ion temperature measurements and fits for a T_{ped} scan. b) fits only for a P_{heat} scan.

2. Experimental Results

The first group of JT-60U discharges [4] used in our tests form four T_{ped} scans (at constant heating power) and a heating power scan (at fixed T_{ped}) in ELMy H-mode discharges with I_p=1.8 MA, B_o=3 T, R_o=3.2 m, a=0.82-0.85 m, κ=1.5, δ=0.16, q_{95}=3, n_e=2.6-3 x10^{19} m^{-3}, Z_{eff}~2.6, and P_{abs}=6-10 MW. All scans have relatively low densities, where a wide range of T_{ped} is observed, but with increasing density the type I ELM boundary reduces the T_{ped} range. The measured ion temperatures from one T_{ped} scan are shown in Fig. 1a, together with least squares fits of the form $T_i = A_1 + A_2r^2 + A_3r^3 + A_4r^4$. Only fits are shown for the power scan in Fig. 1b to avoid obscuration, as all the profiles overlap within 15% as the power is raised by 45% (causing n_e to rise 12%); T_e is constant to within ~10%. Higher power heating frequently produces higher density (and more stored energy) but we have selected plasmas that have a density close to that of the plasmas heated by lower power.

The cause of the T_{ped} variation at fixed P_{heat}, I_p, B_{tor}, etc., is not known. Whatever the cause, we uniformly observe that the core temperatures respond roughly proportionally to changes in the peripheral temperatures, even when there is no change in heating power. In the power scan the pedestal temperature may be clamped by the increasing frequency of type I ELMs at higher powers. This clamping, together with the observed core-pedestal coupling, leads to strong power degradation of energy confinement once the type I ELM boundary has been reached [4].

In idealized circumstances very 'stiff' transport produces a fixed temperature profile shape, scaled in proportion to T_{ped}, but nearly independent of heating power. The constancy of the measured T_i profile shape can be judged from the temperature ratios shown in Fig. 2a, in which T_1=T_i for lower T_{ped}, and T_2=T_i for higher T_{ped}. In ideal circumstances a 'soft' transport model which is independent of T_i and its gradient will predict that core temperatures rise above T_{ped} by an amount which is proportional to the heating power, but independent of T_{ped}. In this case a T_{ped} change at constant heating power produces a

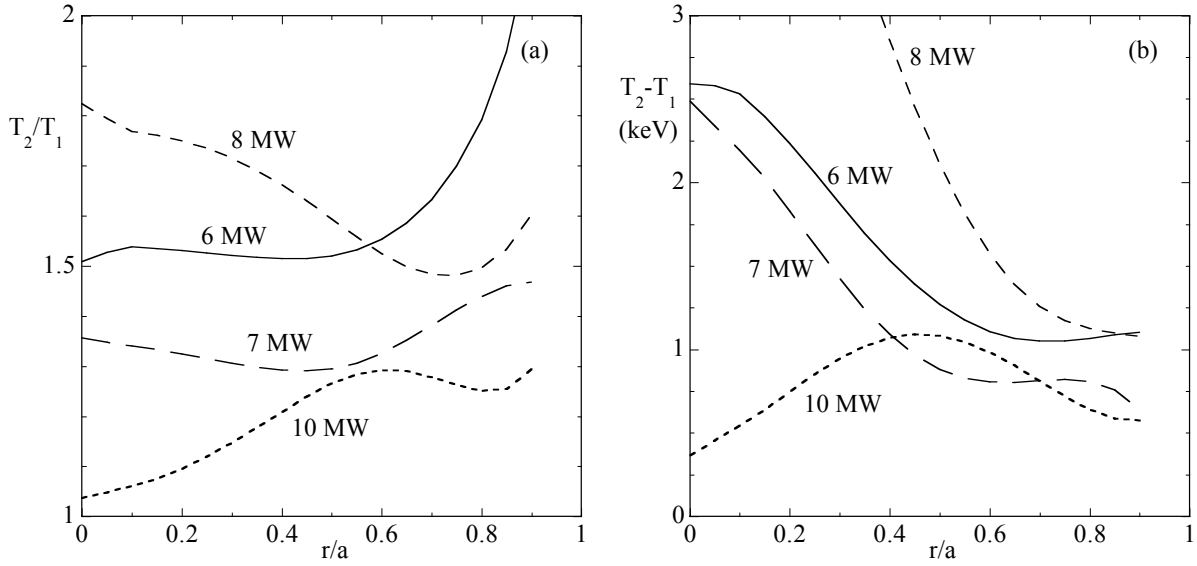

Fig.2. Four T_{ped} scans: a) Temperature ratios and b) temperature differences.

radially constant temperature difference. Fig. 2 shows that these real discharges approach, but do not match, the idealized limit of 'stiff' transport. Moving inwards from the periphery, the ratio T_2/T_1 drops initially and then holds approximately steady. (The outstanding exception - the 8 MW scan - has 30% lower density in the high T_{ped} plasma, which reduces Q_{ie}, and increases the conducted power in the ion channel. In the other scans the density changes no more than 10%.) The periphery thus has relatively 'soft' transport, and approximately constant T_2-T_1, while the core is relatively stiff with approximately constant T_2/T_1.

Central heating power was varied in another group of H-mode discharges by alternately using neutral beams that pass near or avoid the magnetic axis (which was 0.25 m above the midplane). Other discharge parameters are I_p=1.5 MA, B_o=3 T, R_o=3.4 m, a=0.88 m, κ=1.4, δ=0.3, q_{95}=4.3, n_e=2.6x10^{19} m^{-3}, Z_{eff}~2–2.5, and P_{abs}=4.2-5.5 MW. On-axis heating increases the heating power from TOPICS[8]/OFMC[9] by 60% inside a/2 (Fig. 3a); this is

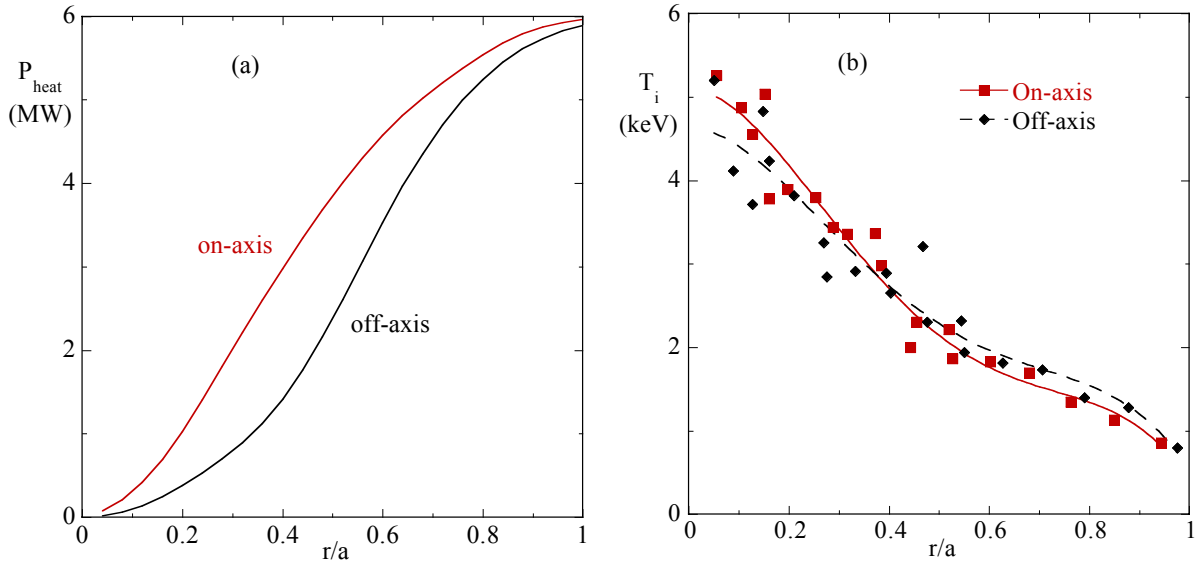

Fig.3. For on-axis (solid) and off-axis (dashed) heating: a) Integrated heating power and b) measured ion temperature profiles

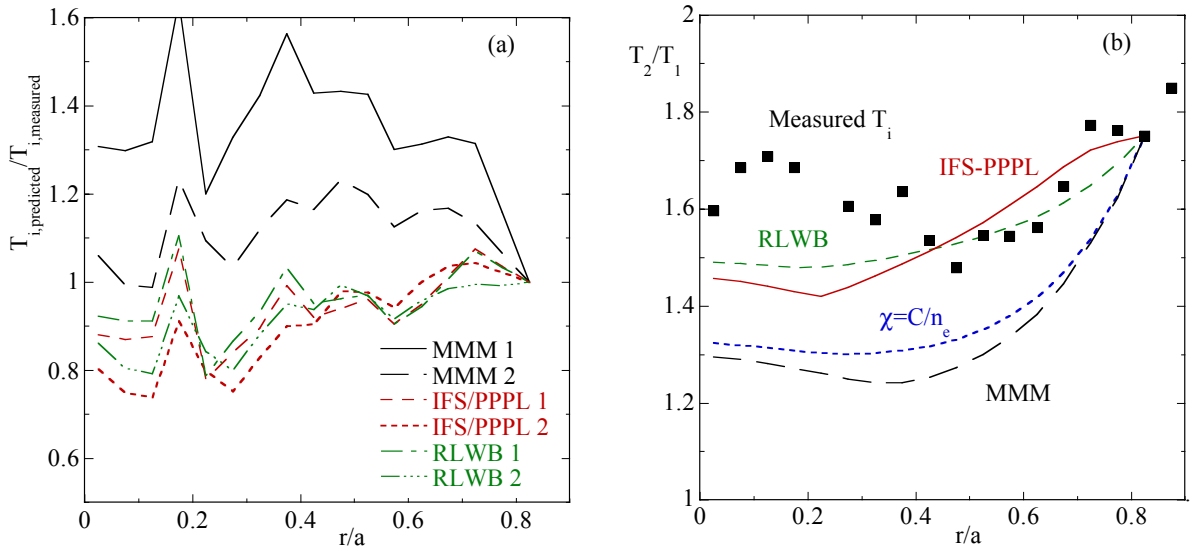

Fig. 4. For a T_{ped} scan with P_{heat}=6 MW: a) the ratio of the predicted to measured T_i, b) the ratio of predicted ion temperatures for discharges with low (1) and high (2) T_{ped}

supported by the measured DD neutron rate increase of 50%. With the extra central heating, the core ion temperature rises by only 10% in the last half of a sawtooth cycle (Fig. 3b). The plasmas with higher central heating do reheat more rapidly after a sawtooth crash, and have central T_i differences of up to 20% in the first half of a sawtooth cycle. The central sawtooth mixing region is somewhat larger than r=0.21 m, the soft X-ray sawtooth inversion radius.

3. Transport Model Predictions

Transport models are tested by solving the electron and ion power balance equations to make temperature predictions for the discharges described above. The iterative solution algorithm uses predicted temperatures and measured $n_e(r)$, Z_{eff}, q(r), etc., to evaluate the transport model diffusivities; measured temperatures are used for the outer boundary condition at r/a=0.82 (the outermost position with reliably measured T_i). The heating profile is calculated by TOPICS[8]/OFMC[9], which includes fast ion losses caused by toroidal field ripple. The tested transport models are the RLWB [10] (with Bohm-like ions and gyro-Bohm electrons), the IFS/PPPL [11], and the Multimode model [5]; the last two are purely gyro-Bohm. An *ad hoc* model with $\chi=C/n_e$ was used as a foil for the others; it represents a 'soft' thermal diffusivity with no dependence on temperatures or their gradients.

Fig. 4a shows the ratio of predicted to measured ion temperatures for discharges at the ends of the T_{ped} scan with P_{heat} = 6 MW; discharge 1 has the lower T_{ped}, 2 has higher T_{ped}. Ignoring the region dominated by sawteeth, r< 0.3a, we find that the RLWB and IFS/PPPL models fit the measured temperatures to within 15%, while the Multimode model's predictions are generally 15-40% too hot. Moreover, Fig. 4b shows the Multimode predictions are 'softer' than those of $\chi=C/n_e$. In some other T_{ped} scans, however, the Multimode model's predictions scale with T_{ped} in a fashion similar to experiment. Nevertheless, Multimode predictions are generally 20-40% too hot; the cause may lie in the periphery, where the Multimode model's ITG component is usually weak. The model with $\chi=C/n_e$ is omitted from Fig.4a because C was chosen to generally fit the data; only this model's T_{ped} scaling (see Fig. 4b) is of real interest. It demonstrates that a very 'soft' transport model does indeed depart from the observed 'multiplicative' enhancement of the temperature across much of the profile

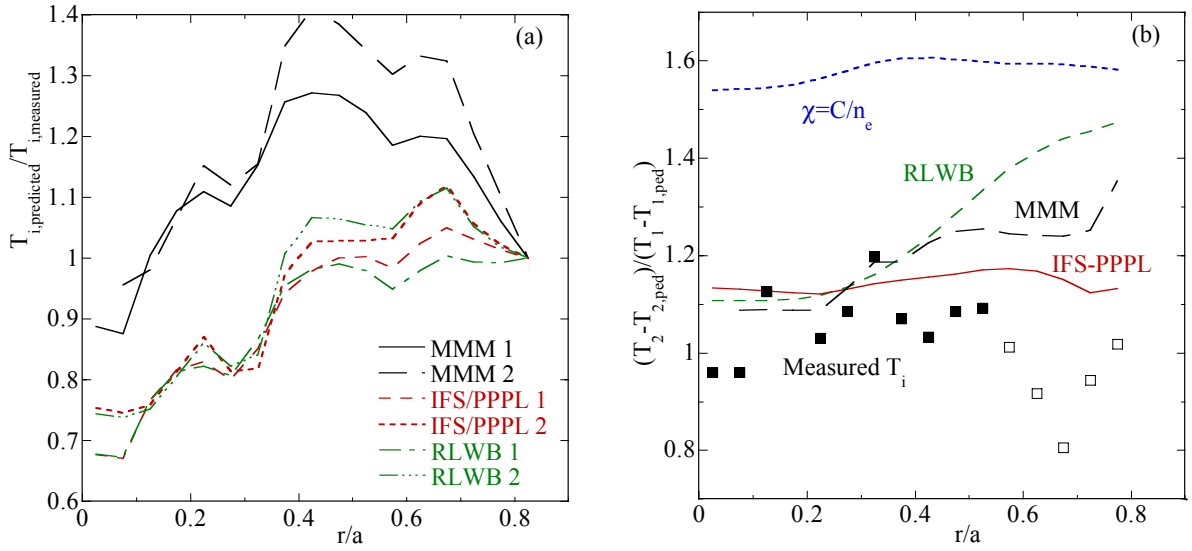

Fig. 5. For a P_{heat} scan with fixed T_{ped}: a) the ratio of the predicted to measured T_i, b) the ratio of predicted T_i-T_{ped} for discharges with low (1) and high (2) P_{heat}.

Predictions for discharges at the ends of the P_{heat} scan with fixed T_{ped} are shown in Fig. 5; discharge 1 has the lower heating power, 2 the higher. As in the T_{ped} scans the RLWB and IFS/PPPL models generally agree with the measured temperatures outside r=0.3a, but the Multimode model's ion temperature predictions are too high (Fig. 5a) except in the sawtooth mixing region, r<0.3a. A measure of the stiffness of the predicted power scaling is shown in Fig. 5b: the predictions with $\chi=C/n_e$ illustrate the expected linear scaling of (T_i-T_{ped}) with heating power. The extremely uncertain experimental values in the outer region are denoted with unfilled symbols; here (T_i-T_{ped}) ~ the uncertainty of T_i. Note that the RLWB model is notably softer than the other models in the region just inside the boundary condition; in spite of this, however, its core temperature predictions are quite acceptable (Fig. 5a). Predictions for the on-axis and off-axis plasmas closely follow the trends described above.

The RLWB and Multimode models' T_{ped} scaling is qualitatively similar to the experimental results in that both models are relatively soft in the periphery but stiffer in the core; however, the Multimode model predictions are generally too hot. While the IFS/PPPL model is very stiff all across the plasma, its predictions are nevertheless generally in agreement with the measurements.

[1] D. R. Mikkelsen, et al., "Tests of 1-D Transport Models, and their Predictions for ITER", in Fusion Energy (Proc. 17th Intl. Conf., Yokohama, 1998) CN-69/ITERP1/08.
[2] ITER Physics Basis, Chapter 2.8, Nucl. Fusion **39** (1999) 2215-2225.
[3] N. Asakura, et al., Plasma Phys. Control. Fusion, **39** (1997) 1295-1314.
[4] H. Urano, et al., submitted to Plasma Phys. Control. Fusion, 2000.
[5] J. E. Kinsey, R. E. Waltz, and J. C. DeBoo, Phys. Plasmas, **6** (1999) 1865-1871.
[6] W. Suttrop, et al., Plasma Phys. Control. Fusion, **39** (1997) 2051–2066.
[7] M. Greenwald, et al., Plasma Phys. Control. Fusion, **40** (1998) 789–792.
[8] H. Shirai, et al., J. Phys. Soc. Japan, **64** (1995) 4209.
[9] K. Tani, M. Azumi, H. Kishimoto, and S. Tamura, J. Phys. Soc. Japan, **50** (1981) 1726.
[10] M. N. Rosenbluth, et al., in Fusion Energy (Proc. 15th Intl. Conf., Seville, 1994) **2**, 517.
[11] M. Kotschenreuther, et al., Phys. Plasmas, **2** (1995) 2381.